available at www.sciencedirect.com

ScienceDirect

journal homepage: www.elsevier.com/locate/compag

Field comparison of two prototype soil strength profile sensors

Kenneth A. Sudduth[a,*], *Sun-Ok Chung*[b], *Pedro Andrade-Sanchez*[c], *Shrinivasa K. Upadhyaya*[d]

[a] *USDA Agricultural Research Service, Cropping Systems and Water Quality Research Unit, 269 Agric. Engineering Bldg., University of Missouri, Columbia, MO 65211, USA*
[b] *Department of Bioindustrial Machinery Engineering, Chungnam National University, Daejeon 305-764, Republic of Korea*
[c] *Maricopa Agricultural Center, University of Arizona, Maricopa, AZ 85239, USA*
[d] *Department of Biological and Agricultural Engineering, University of California, Davis, CA 95616, USA*

ARTICLE INFO

Article history:
Received in revised form
20 November 2006
Accepted 21 November 2006

Keywords:
Soil compaction
Soil strength
Precision agriculture
Sensors
Cone index

ABSTRACT

Soil compaction that is induced by tillage and traction is an ongoing concern in crop production, and also has environmental consequences. Although cone penetrometers provide standardized compaction measurements, the pointwise data collected makes it difficult to obtain enough data to represent within-field variability. Moreover, penetrometer data exhibit considerable variability even at a single location, requiring several measurements to obtain representative readings. For more efficient data collection, on-the-go compaction sensors that obtain data at multiple depths are being developed by several research groups. The objective of this research was to evaluate and compare the field performance of two on-the-go compaction sensors. Tests were conducted at two central Missouri field sites where soil types ranged from sandy loam to clay. The soil strength profile sensor (SSPS) measured compaction to a 50-cm depth on 10-cm intervals. The soil compaction profile sensor (SCPS) also used five sensing elements and obtained data to 40.6 cm on a 7.6-cm interval. Cone penetrometer measurements of compaction were obtained at intervals along each transect for comparison. Data were compared between the two on-the-go sensors and were also related to penetrometer and soil property data. The repeatability of SCPS data was somewhat better than that of SSPS data. Data from the two sensors were linearly related, with similar regression equations for each individual site and for both sites combined. The agreement between SCPS and SSPS data ($r^2 = 0.56$ over all sites and depths) was much better than between sensor and penetrometer data ($r^2 = 0.19$–0.20). Maps of SCPS and SSPS data for a 13.5-ha field site showed very similar patterns. Maps of penetrometer data were also similar to those of on-the-go sensor data, but showed fewer spatial details. Variation in soil strength appeared to be primarily related to variations in soil physical properties (e.g., texture, water content). Due to the similarity between SCPS and SSPS data, we conclude that measurements obtained with the two on-the-go soil sensors were affected similarly by soil strength variations within the study sites. Side-by-side comparison of the on-the-go sensors

* *Corresponding author*. Tel.: +1 573 882 4090; fax: +1 573 882 1115.
E-mail address: Ken.Sudduth@ars.usda.gov (K.A. Sudduth).

Abbreviations: CI, cone index; DGPS, differential global positioning system; EC_a, soil apparent electrical conductivity; SCPS, soil compaction profile sensor; S.D., standard difference; S.E., standard error; SSPS, soil strength profile sensor

0168-1699/$ – see front matter © 2007 Elsevier B.V. All rights reserved.
doi:10.1016/j.compag.2006.11.006

provided a convenient approach to validate sensor performance. The study also provided information to improve on-the-go sensor design and to relate sensor data to other measures of soil compaction.

© 2007 Elsevier B.V. All rights reserved.

1. Introduction

Soil compaction caused by wheel traffic of large agricultural machinery and/or tillage operations, as well as due to natural phenomena, is a concern in crop production and the environment. When soil is compacted, there are changes in soil physical properties such as soil structure, consistency (cohesion and adhesion), pore space, and density, which play an important role in the growth and development of plants. Soil compaction can have deleterious effects on crop growing conditions and the environment (Soane and Van Ouwerkerk, 1995); effects which are difficult to remediate. Because it is difficult to measure compaction *in situ*, a common approach is to measure soil strength, a parameter that is strongly associated with compactness, packing density, relative bulk density, and drainable porosity (Canarache, 1991).

The cone penetrometer is the tool most often used to quantify soil strength *in situ* (Mulqueen et al., 1977; Perumpral, 1987). The index of soil strength measured by a cone penetrometer, cone index (CI), is defined as the force per unit base area required to push the penetrometer through a specified small increment of depth at a standard insertion rate (ASAE, 2005a,b). In general, CI varies greatly with depth in the rooting zone, and is affected by soil properties such as water content, bulk density, and particle size distribution (e.g., clay content) (Perumpral, 1987; Elbanna and Witney, 1987; Guerif, 1994). Perumpral (1987) stated that CI increased with increasing soil density and decreasing soil water content. Elbanna and Witney (1987) expressed CI at an average tillage depth as a function of clay fraction, cohesive and frictional coefficients, soil water content, and soil specific weight.

Cone penetrometer readings require a "stop-and-go" procedure with data collected at discrete locations, making it difficult to collect enough data to accurately map compaction variations within a field. Additionally, penetrometer data are highly variable even at a single location and require several readings to obtain representative measurements. Even in non-spatial analyses, researchers have often collected hundreds of penetrometer readings to investigate treatment differences (Busscher et al., 1986) and to relate cone index to soil properties such as water content and bulk density (Sojka et al., 2001).

To make data collection more efficient, a number of researchers have attempted continuous, "on-the-go" measurement of soil strength. Glancey et al. (1989) developed an instrumented chisel using a strain gauge array. Evaluation of this instrument (Glancey et al., 1996) showed that force distribution over the tillage depth was linear at a shallow operating depth (153 mm) in both tilled and untilled soils. However, the distribution was non-linear at a greater depth of operation (305 mm) in untilled soil. Adamchuk et al. (2001) used a similar approach when instrumenting a vertical blade with an array of four strain gauges to predict soil cutting-force distribution over the tool operating depth.

Alihamsyah et al. (1990) developed a horizontally operated penetrometer and evaluated the effect of tip geometry, apex angle, and extension, along with operating speed. Measurements obtained using a prismatic tip with an apex angle of 30° related well to CI. Chukwu and Bowers (2005) modified this device so that it could measure soil mechanical impedance at three depths simultaneously. They utilized three prismatic tips with a 30° apex angle and three load cells similar to the one used in the single tip sensor. A 10-cm vertical tip spacing was chosen to provide a 30-cm sensing profile and to minimize measurement interference from one tip to the next. When operated at a speed of 0.03 m s^{-1} through soil layered with different compaction levels, the sensor detected the difference in soil mechanical impedance with depth at a 5% significance level.

Hall and Raper (2005) developed a device consisting of a single sensor mounted on the leading edge of a tine and a reciprocating drive for oscillating the tine up and down while it moved horizontally through the soil. They used 30° prismatic sensing tips and defined a "wedge index" as the measured force divided by the base area of the tip. When using a 6.25 cm^2 wedge tip, CI was 1.52 times greater than the wedge index with an r^2 of 0.65. When the base area of the tip was increased to 25 cm^2, the slope of the relationship increased to 2.99 ($r^2 = 0.83$). They stated that an absolute equation to relate the wedge index and CI measurements might not be possible, since both measurement methods were empirical and were affected differently by different soil factors.

Andrade-Sanchez et al. (2007) developed a soil cutting-force profile sensor that could take measurements to a 63-cm depth on 7.5-cm increments (5-cm active cutting elements separated by 2.5-cm dummy elements). The device consisted of eight cutting edges supported by independent load cells that measured the force on each cutting edge as the system was pulled through the soil. Soil cutting force was influenced by soil water content, depth of operation of the tine, and location of the cutting edge. Later evaluation of the sensor showed that the effect of operating speed on cutting force was not significant between 0.65 and 1.25 m s^{-1} and that the sensor output could be expressed as a function of CI and operating depth with a coefficient of multiple determination of 0.985 (Andrade-Sanchez et al., 2007).

Chung et al. (2006) developed a sensor that measured soil strength to a 50-cm depth on 10-cm increments. Cutting forces of five prismatic tips extended in front of a main blade were measured by load cells as the tractor-mounted device moved through the soil. Field research (Chung et al., 2004) showed that soil strength measured by this sensor was a function of water content, bulk density, and texture. Best results were obtained when depth of operation was included in the model or when analysis was conducted within a single depth.

The performance of each of the sensors described above has generally been evaluated with respect to standard CI measurements. However, such a comparison can be problematic

because a number of factors related to soil strength may affect data obtained by on-the-go sensors and vertical penetrometers differently. Even if the soil encountered by a penetrometer and an on-the-go sensor exhibited the same conditions (e.g., bulk density, water content, texture, internal friction angle, and cohesion), differences in tool design (e.g., geometry and surface roughness) and operation (e.g., speed and depth of operation, and horizontal vs. vertical direction of movement) would likely cause measured strength values to be different. In addition to being encountered in practice (e.g., Andrade-Sanchez et al., 2007; Chung et al., 2004; Hall and Raper, 2005), these differences can also be predicted with soil strength models (Chung and Sudduth, 2006).

Operational factors are also important when comparing soil strength measurements within a sensor type (i.e., horizontal on-the-go sensor or vertical cone penetrometer). McKyes (1985) stated that the dynamic effects of a sensor moving through the soil included both inertia forces due to accelerating the soil volume and changes in soil strength at a high rate of shear. He also stated that the effect of shear rate was not significant in purely frictional soils, but was significant in clay soils, outweighing the inertia forces. It is generally accepted that the soil force acting on a tool body increases approximately with the square of speed (Stafford, 1979; Wheeler and Godwin, 1996). Schuring and Emori (1964) found a critical speed, below which the effects of operating speed would not be significant. For the tool widths used in soil strength sensors, this critical speed would be in the approximate range of 0.5–1.5 m s^{-1}.

Operating depth also affects soil strength due to differences in soil conditions and the soil failure mechanism along the soil profile. Sojka et al. (2001) related cone index to water content and bulk density of a silt loam soil. The relationship was poor when derived from full-profile datasets but improved when data were segregated by depth. Luth and Wismer (1971) tested flat soil cutting blades in a sandy soil and found that the force increased linearly as depth increased for a wide blade but the force–depth curve increased as a squared function for narrow blades. When the blades were tested in a clay soil (Wismer and Luth, 1972), force was related to depth by a power less than one for wide blades and by a power equal to or less than one for narrow blades. Godwin and Spoor (1977) noted that above a certain depth, soil displaced by a horizontally moving tine would move upward, forward, and sideways (crescent failure). Below this depth, only forward and sideways displacement (lateral failure) would occur. In comparison, the failure mode experienced by a cone penetrometer would be similar over all depths below the depth where the soil failure pattern becomes fully developed (Chung and Sudduth, 2006). Thus, there is an inherent depth dependency in the relationship of measured soil failure forces.

1.1. *Objective*

Because of the difficulties described above in validating on-the-go soil strength data with respect to CI, our overall objective was to validate the operation of two prototype soil strength sensors through a side-by-side field comparison. Specific objectives included:

- Documenting the repeatability of on-the-go sensor data,
- Relating data from each on-the-go sensor to CI, and
- Comparing soil strength measurements obtained with the two sensors.

2. Materials and methods

2.1. *University of California-Davis soil compaction profile sensor (SCPS)*

The design of the current version of the SCPS (Fig. 1; Andrade et al., 2004) was based on experience gained from extensive field testing of a previous prototype (Andrade-Sanchez et al., 2007). The thickness of the shank was reduced to 2.7 cm from over 5 cm so that the sensor was similar in dimension to a subsoiler shank or chisel. The rake angle of the device was changed to 90° (a vertical shank) to aid in self-penetration of the device into ground. Force sensing was accomplished with five customized octagonal ring load-sensing units instrumented with four strain gauges each (Fig. 1, right). The wedge-shaped sensing elements were 6.4 cm high and 2.7 cm wide, with a 1.3 cm vertical separation between elements. Three different sizes of force transducer were used, with dimensions calculated on the basis of the expected magnitude of forces according to their depth in the soil profile. Expected forces were estimated from field test results obtained using the previous prototype of the SCPS. An overload protection mechanism consisting of disc springs was designed to become active when the force reached rated capacity. The sensing elements were individually calibrated and followed a linear relationship between the applied static load and sensor output. Table 1 presents load specifications and locations for each of the cutting element/force sensing assemblies of the SCPS as operated in these field tests.

For field data collection, the load cells were connected to a Campbell Scientific[1] CR23X (Logan, Utah) data acquisition system that was set to scan the output of all five load cells and accessory instruments at a sampling frequency of 5 Hz. The data acquisition system also acquired position data from a DGPS receiver. Force data were later averaged to 1 Hz for analysis.

2.2. *USDA-ARS/University of Missouri soil strength profile sensor (SSPS)*

The Missouri SSPS (Fig. 2) provided soil strength data at nominal center depths of 10, 20, 30, 40, and 50 cm below the soil surface. The five prismatic force-sensing tips (1.9 cm high by 1.9 cm wide) extended 5.1 cm ahead of the main blade to minimize effects of soil movement by the main blade on sensed soil strength. Thus, significant design differences existed between the two sensors in the size of the sensing element, the spacing between the elements, and the extension of the cutting tips in front of the main support blade. For the SSPS, the force on each tip was measured by a miniaturized load cell with a

[1] Mention of trade names or commercial products is solely for the purpose of providing specific information and does not imply recommendation or endorsement by the U.S. Department of Agriculture or its cooperators.

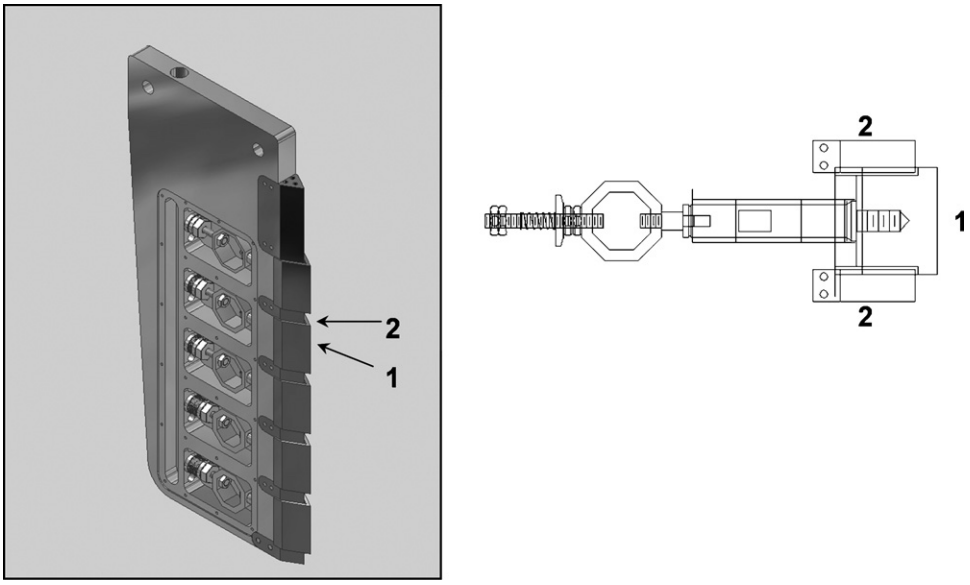

Fig. 1 – Structure of the SCPS developed at the University of California-Davis: overall view of 2.7-cm wide cutting shank (left), and expanded view of force-sensing components (right), including (1) 6.4-cm high active cutting elements spaced 1.3 cm apart by (2) dummy elements.

7 kN dynamic load capacity located in the main blade and in contact with the rear end of the tip shaft. Prior to field tests all load cells were calibrated to a single linear relationship between static applied load and sensor output (Chung et al., 2006). Load cell outputs were recorded at 10 Hz on a laptop computer-based data acquisition system and later averaged to 1 Hz. Additional details of SSPS design are given in Chung et al. (2006), and sensing element capacities and locations are given in Table 1.

2.3. *Field sites*

The sensors were compared at two research sites: site 1 (13.5 ha) near Centralia, Missouri (39.230 N, 92.117 W) and site 2 (4.5 ha) near Hartsburg, Missouri (38.753 N, 92.384 W). The sites were located within fields managed in corn–soybean rotations. The soils found at site 1 were of the Mexico series (fine, smectitic, mesic aeric Vertic Epiaqualfs) and the Adco series (fine, smectitic, mesic aeric Vertic Albaqualfs). Surface textures of these somewhat poorly drained soils ranged from silt loam to silty clay loam. The subsoil claypan horizon(s) were silty clay loam, silty clay, or clay, with 50–60% smectitic clay. Topsoil depth above the claypan (depth to the first Bt horizon) ranged from less than 10 cm to greater than 100 cm (Sudduth et al., 2003). The alluvial soils at site 2 in the Missouri River flood plain were mostly of the Leta series (clayey over loamy, smectitic, mesic Fluvaquentic Hapludolls) and Haynie series (clayey over loamy, smectitic, mesic Fluvaquentic Hapludolls). A few areas within this field site had no soil series name assigned but were classified as being 'sand over sand'. These sand depositional areas resulted from flooding in 1993 when the Missouri River levees failed.

2.4. *Data collection and processing*

Data were collected after corn harvest in 2003 on a nominal 30-m transect spacing for site 1 and a 20-m transect spacing for site 2. The direction of data collection was slightly angled (about 5 degrees) with respect to the harvested crop row to minimize effects of possible systematic patterns of soil strength due to past crop and field management practices. The nominal operating speed of the SSPS was 1.5 m s^{-1}; the average

Table 1 – Load capacity and depth position of SCPS and SSPS cutting elements

Cutting element number	University of California-Davis SCPS			USDA-ARS/University of Missouri SSPS		
	Rated capacity (kN)	Cutting element depth		Rated capacity (kN)	Cutting element depth	
		Center depth (cm)	Depth range (cm)		Center depth (cm)	Depth range (cm)
1 (top)	1.1	6.4	3.2–9.5	7.0	10	9–11
2	2.2	14.0	10.8–17.1	7.0	20	19–21
3	2.2	21.6	18.4–24.8	7.0	30	29–31
4	4.5	29.2	26.0–32.4	7.0	40	39–41
5	4.5	36.8	33.6–40.0	7.0	50	49–51

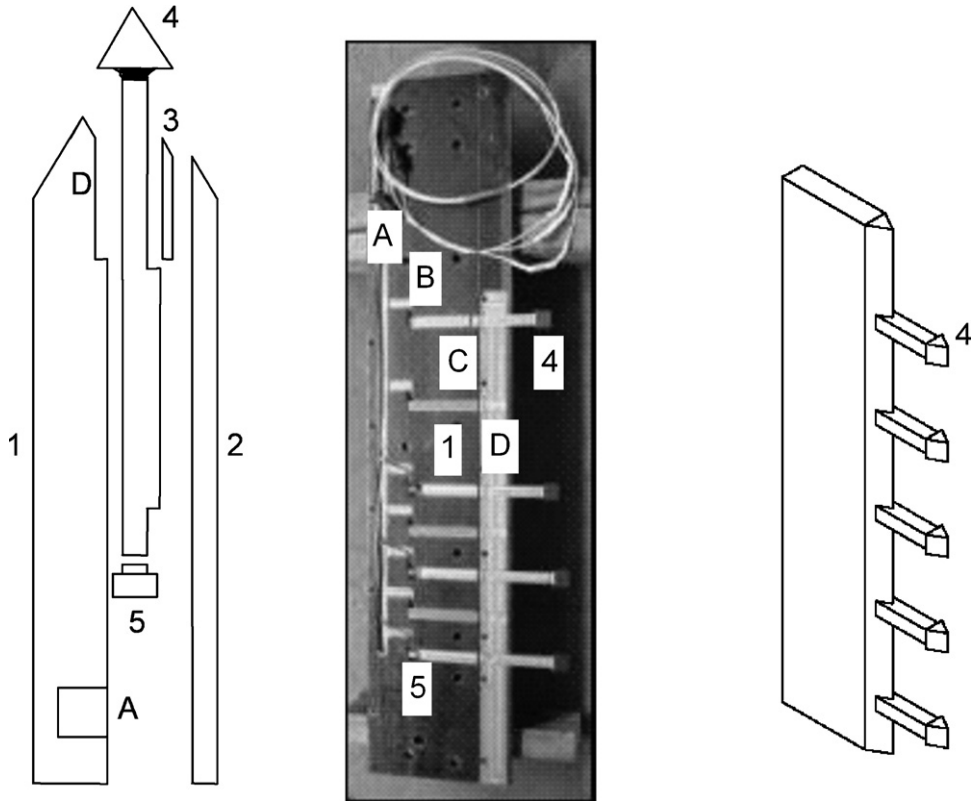

Fig. 2 – Structure of the SSPS developed by USDA-ARS and the University of Missouri: top view (left), side view of the body plate (center), and isometric view (right). Components include: (1) body plate, (2) cover plate, (3) retaining bar, (4) prismatic tip with 1.9 cm × 1.9 cm base area, and (5) load cell. Parts of the body plate include: (A) wiring tunnel, (B) holes for load cells, (C) grooves for prismatic tips, and (D) groove for retaining bar.

operating speed of the SCPS was 1.65 m s^{-1}. The combination of operating speed and sampling rate ensured that multiple (>3) data points would be obtained within the 1- to 2-m range in spatial dependence determined for CI data in previous research on one of these fields (Chung and Sudduth, 2004). The tractor-mounted support frames for each sensor were equipped with gauge wheels to maintain a constant depth of operation. At site 2, additional transects (test transects) were made in the opposite direction of travel and parallel to the first set of transects (reference transects) to evaluate repeatability of each sensor measurement. Distances between the reference and test transects were less than 3 m, but no closer than 1 m. Position information for all field data collection was obtained using DGPS receivers with 1-m or better accuracy specifications.

Sensor position data were corrected considering the direction of travel and the offset between the DGPS antenna and the strength sensor. Appropriate calibration factors were used to convert sensor outputs to a prismatic soil strength index (PSSI). As an analog to the commonly used penetrometer CI, PSSI was defined as the force on the sensing tip divided by the base area of the prismatic wedge. For comparison between sensors and with CI, PSSI values were averaged over a 15-m radius from each CI measurement site. Thus, each sensor reading used for statistical comparison was a 30-m average along the measurement transect.

CI profiles were obtained with an ASAE-standard small cone penetrometer (ASAE, 2005a) on a 30-m interval along each transect. At each location (133 at site 1 and 52 at site 2), triplicate CI profiles obtained within 1 m were averaged to represent soil strength as a function of depth. A non-standard penetration rate of 40 mm s^{-1} was used; however, prior research (Sudduth et al., 2004) showed no significant difference in CI between this rate and the standard 30 mm s^{-1}. The CI data were collected between the SSPS and SCPS transects, such that the distance to each of the sensor runs was approximately equal. For analysis, 5-cm-depth-averaged CI values were calculated centered on each SSPS measurement depth (i.e., 10, 20, 30, 40, and 50 cm).

Because SCPS and SSPS sensing depths were different, it was necessary to create a comparison dataset. Although we recognize that soil strength generally varies non-linearly as a function of depth, we assumed that variation over a small depth increment could be reasonably approximated by a straight line. Thus, a synthetic 10-cm depth reading for the SCPS was constructed by averaging data from the 6- and 14-cm depth elements. Similarly, we constructed a 35-cm depth reading for the SSPS by averaging data from the 30- and 40-cm depth elements. A 35-cm-depth CI reading was constructed from the 30- and 40-cm depth CI readings. The center depths of the data in the comparison dataset differed by at most 2 cm (Table 2).

Table 2 – Soil strength dataset constructed to allow comparison of data from SCPS and SSPS

Nominal depth (cm)	Raw sensor center measurement depths used in constructing comparison dataset (cm)	
	SCPS data	SSPS data
10	Mean of 6.4 and 14.0 = 10.2	10
20	21.6	20
30	29.2	30
35	36.8	Mean of 30 and 40 = 35

At every second CI collection location (52 locations at site 1 and 25 locations at site 2), 4-cm-diameter soil cores were obtained and segmented into five 10-cm-long depth intervals centered on the PSSI measurements (i.e., 5–15 cm, 15–25 cm, 25–35 cm, 35–45 cm, 45–55 cm) for gravimetric determination of soil water content.

To provide an indication of soil textural differences within the field sites, apparent soil electrical conductivity (EC_a) data were measured with a Veris Model 3100 sensor on transects parallel to PSSI data collection. Transects were 10 m apart and EC_a data were obtained at a 4- to 6-m spacing along each transect. EC_a measurements are primarily dependent on soil texture and soil water content in non-saline soils, and have been used to differentiate soil types and soil conditions (e.g., bulk density and clay fraction; Johnson et al., 2001). Higher EC_a values indicate greater soil clay fractions (or smaller sand fractions) than those with low EC_a values (Sudduth et al., 2003).

2.5. *Data analysis*

Separate analyses were carried out to evaluate the repeatability of the SSPS and SCPS data; to compare SSPS, SCPS, and CI data; and to develop and evaluate field-scale PSSI maps. Repeatability of soil strength measurements obtained with the SSPS and SCPS was evaluated by comparing PSSI measurements obtained from the test transects at site 2 with those from the corresponding reference transects. The 30-m-averaged data for each of the five measurement depths ($n = 250$) were used in the comparison for each sensor. Linear regression through the origin was used to relate test transect readings to reference transect readings.

Summary statistics and Pearson correlation coefficients were calculated to compare SCPS, SSPS, and CI data. Additional comparisons were carried out using linear regression analysis between sensor datasets.

Maps of soil strength, quantified as PSSI, were developed from each of the two sensors for site 1. Site 1 was chosen for this exercise because its aspect ratio (closer to 1:1) made it more amenable to mapping than site 2. Sensor transect data (1 Hz data on a 30-m transect spacing) were interpolated to 10-m grids for mapping. A separate equal-area color scale was used for the map representing each sensor–depth combination.

3. Results and discussion

Data from a short section of an example data collection transect are shown in Fig. 3. Similarities in data patterns between the two sensors included higher forces near the beginning of the example transect and comparable relative variations in force level over short distances. Considerably lower forces were observed with the SSPS, due to its smaller sensing elements.

3.1. *Repeatability of sensor data*

Strength (PSSI) data from the test transects were strongly related to those from the reference transects, and were distributed around the 1:1 line for each sensor (Fig. 4). The paired transect data for the SCPS were more strongly related ($r^2 = 0.86$) than those for the SSPS ($r^2 = 0.70$). On the other hand, the central tendency of the relationship was slightly closer to the 1:1 line for the SSPS (slope = 0.95) than for the SCPS (slope = 0.91). The results of this comparison gave us confidence in the repeatability of the sensor data. Because the slope of each regression was close to 1, the standard error (S.E.) of the

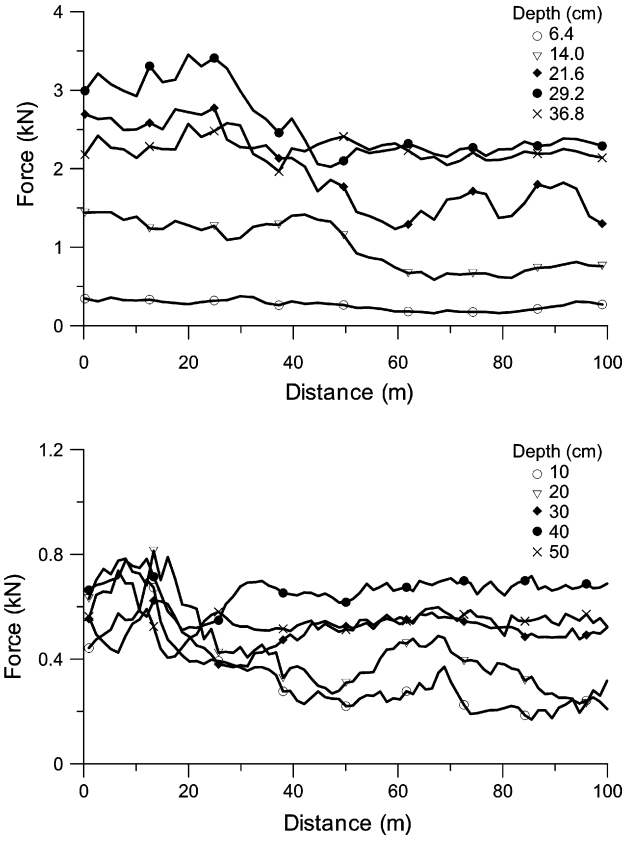

Fig. 3 – Example plot of sensor force measurements at the five sensing depths for soil compaction profile sensor (SCPS, top) and soil strength profile sensor (SSPS, bottom).

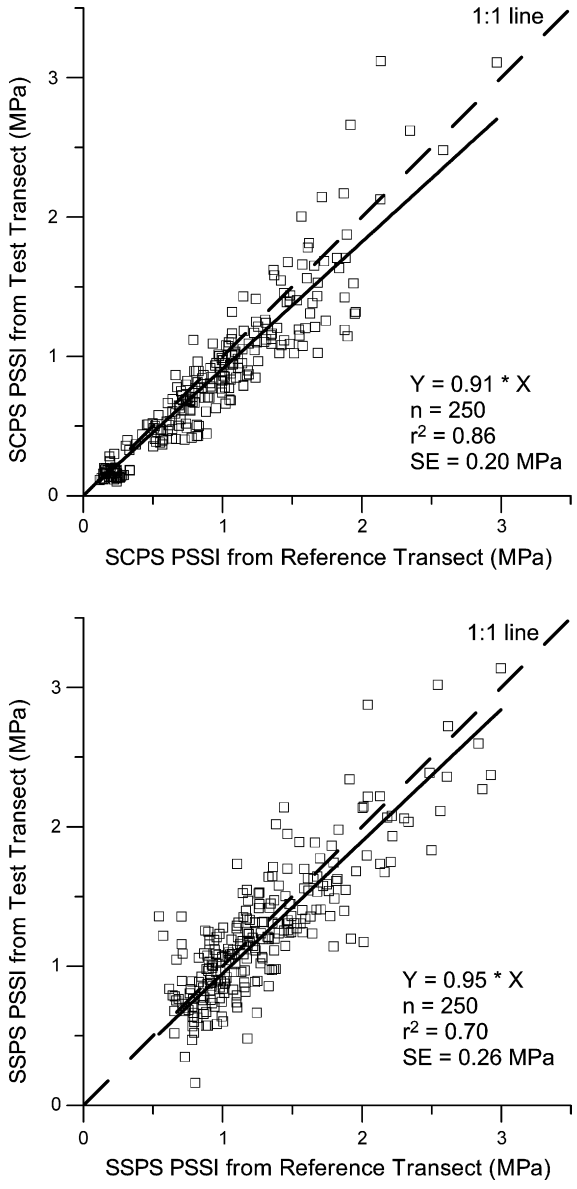

Fig. 4 – Comparison of soil strength data (PSSI) from test and reference transects at site 2 for soil compaction profile sensor (SCPS, top) and soil strength profile sensor (SSPS, bottom).

regression estimate was only slightly lower than the standard difference (S.D.) calculated between the two measurement transects for each sensor (SSPS: S.D. = 0.27 MPa, S.E. = 0.26 MPa; SCPS: S.D. = 0.22 MPa, S.E. = 0.20 MPa). These measures of PSSI variability provided a benchmark against which to judge subsequent between-sensor comparisons.

Examination of the scatter plots (Fig. 4) for the two sensors revealed that differences between the two sets of transects were more proportional to force levels for the SCPS, while the differences with the SSPS were more constant across the range of forces. The better agreement between SCPS transects at lower force levels may have been caused by differences in sensor designs. The larger sensing tips of the SCPS as compared to the SSPS (17.3 cm^2 and 3.6 cm^2 base area, respectively) would provide more averaging, reducing the effect of small-scale soil variation on the overall readings. Also, the rated capacities of the custom-fabricated sensing elements in the SCPS were tailored to expected loads, with the capacity of the shallower sensing elements reduced in comparison to the deeper elements (Table 1). On the other hand, the SSPS was constructed with identical commercial load cells that had a capacity in excess of what was needed for this application. As a consequence, when converted to PSSI, the manufacturer's accuracy specification of 0.14 MPa for these load cells could have resulted in an inherent inaccuracy and would have contributed to the larger S.E. Future refinement of the SSPS design should consider selection of lower-capacity load cells for the shallower depths where lower maximum loads are expected.

3.2. *Comparison of SCPS, SSPS, and CI data*

Table 3 presents summary statistics for sensor and soil water content data obtained at the two test sites. In general, PSSI measured by the SSPS was somewhat larger than that measured by the SCPS (Fig. 5), perhaps due to the differences in sensing geometry between the two devices. Variability in PSSI was also greater for the SSPS at most site–depth combinations. CI was generally higher than PSSI for most site–depth combinations (Fig. 6). Across all depths and two field sites, the overall relationship of data from the two on-the-go sensors was considerably better ($r^2 = 0.56$; Fig. 5) than the relationship of data from either on-the-go sensor to CI ($r^2 = 0.19$–0.20; Fig. 6). This same trend was also seen within the individual sites, as confirmed by correlation values presented in Table 4.

Results were more mixed when considering relationships within a single depth (Table 4). At site 1, CI correlations were lower than between-sensor correlations at shallower depths,

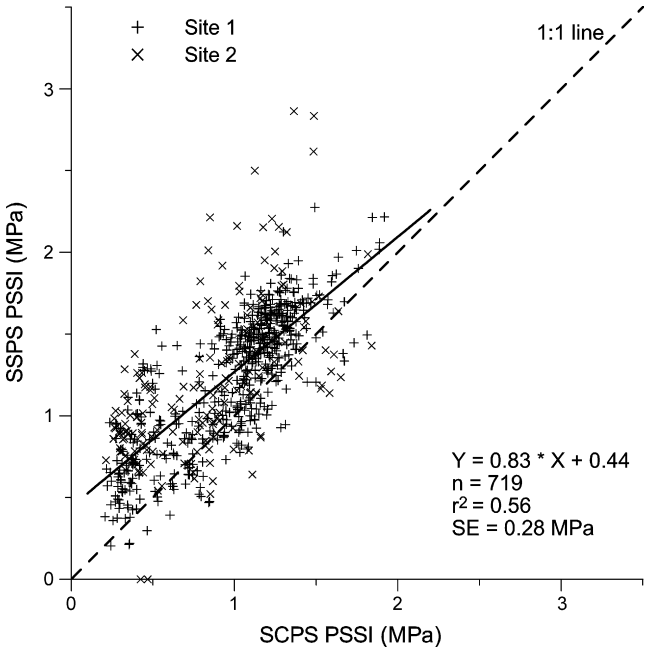

Fig. 5 – Comparison of soil strength data (PSSI) obtained with soil compaction profile sensor (SCPS) and soil strength profile sensor (SSPS). Data include all comparison depths and two test sites.

Table 3 – Descriptive statistics for PSSI, CI, and mass water content (WC) data obtained at the two field sites

Nominal depth (cm)	Sensor data							Soil data		
	SCPS PSSI (MPa)		SSPS PSSI (MPa)		CI (MPa)			WC (%)		
	Mean	S.D.	Mean	S.D.	Mean	S.D.	*n*	Mean	S.D.	*n*
Site 1										
10	0.42	0.13	0.76	0.29	1.11	0.36	132	24.6	1.1	51
20	1.00	0.20	1.04	0.29	1.62	0.53	132	28.1	4.9	51
30	1.24	0.20	1.46	0.20	1.44	0.44	132	32.9	5.1	51
35	1.21	0.18	1.60	0.16	1.37	0.34	132	32.6	3.8	51
Site 2										
10	0.38	0.08	0.84	0.24	1.00	0.52	52	20.2	4.5	25
20	0.78	0.21	0.98	0.22	1.17	0.52	52	20.8	5.0	25
30	1.06	0.19	1.63	0.42	1.67	0.82	52	23.7	4.5	25
35	1.35	0.23	1.53	0.32	1.65	0.52	35	25.2	4.1	17

while they were more similar at deeper depths. Variations in behavior at different depths may have been due to the different mechanisms of soil failure between vertical and horizontal penetration. For a horizontally moving tine, crescent failure occurs above some depth, with soil moving upward, forward, and sideways, while below this depth only forward and sideways displacement occurs. With a tine of 2.54 cm width, similar to the width of the SCPS and SSPS, Godwin and Spoor (1977) found that crescent failure occurred within 12 cm of the soil surface. Thus, the uppermost elements of our sensors would have measured a lower PSSI due to crescent failure. Comparison of the mean values in Table 3 suggests that the crescent failure effect was more prevalent for the SCPS. This result may have been due to the shallower operating depth of the first SCPS sensing element and/or the closer proximity of the SCPS sensing elements to the main support blade. Non-linearity of the PSSI–depth relationship near the surface may have been another contributing factor, since the shallowest SCPS depth was synthesized by averaging two actual measurements (Table 2).

At site 2, generally poorer agreement was seen between the datasets (Table 4). Insignificant or negative correlations were found for all data pairs at the shallowest two depths. For the

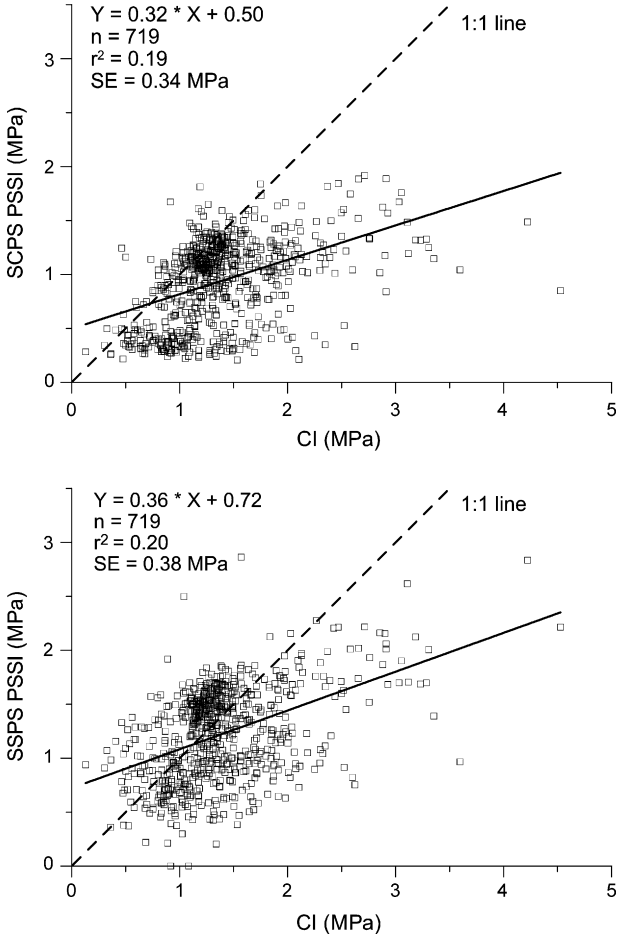

Fig. 6 – Comparison of soil strength data (PSSI) obtained with soil compaction profile sensor (SCPS, top) and soil strength profile sensor (SSPS, bottom) to cone index (CI). Data include all comparison depths and two test sites.

Table 4 – Correlations between data from the SCPS and SSPS sensors, and between data from each sensor and CI

Nominal depth (cm)	Pearson correlation coefficient		
	SCPS vs. SSPS	SCPS vs. CI	SSPS vs. CI
Both sites			
All	0.75	0.44	0.45
10	0.28	0.10	0.13
20	0.47	0.50	0.43
30	0.32	0.32	0.62
35	0.34	0.48	0.60
Site 1			
All	0.82	0.46	0.37
10	0.43	NS[a]	0.27
20	0.69	0.49	0.51
30	0.59	0.59	0.57
35	0.67	0.60	0.58
Site 2			
All	0.61	0.42	0.58
10	−0.32	NS	NS
20	NS	NS	NS
30	0.39	NS	0.62
35	NS	NS	0.80

[a] NS denotes non-significant ($P \leq 0.05$) correlation.

two greater depths, relatively strong correlations were seen between SSPS PSSI and CI. Correlations were not significant between SCPS PSSI and CI, and were different for the two on-the-go sensors. This poorer agreement at site 2 may have been due to more spatial (both horizontal and vertical) variation in soil properties. The alluvial soils at this site were formed and worked by repeated flooding of the nearby Missouri River. In such soils, layers of material having different textures were often deposited in patterns defined by the movement of flood water over the landscape. As such occurrences repeated over time, the structure of the soil became quite complex. Because of the differences in thicknesses and depth locations of the sensing elements of the SCPS and SSPS, the two sensors may have encountered soil layers of different textures, and therefore different strength characteristics. This effect would have been further exacerbated by the spatial separation, and resulting potential for increased soil variation, between the sensing transects.

The central tendency of the relationship between SSPS and SCPS data was similar between the two field sites, but there was more scatter in the relationship at site 2 (Fig. 5, Table 5). Although the between-sensor S.E. (Table 5) provided a measure of agreement between SCPS and SSPS data, this statistic also included the effect of field variability (i.e., the difference in soil conditions between the locations of the two paired measurements). This difference in soil conditions was also reflected in the variability (as S.D.) of the individual sensor measurements discussed in Section 3.1 above. Comparing these statistics for site 2 (no within-sensor data were available for site 1), the between-sensor S.E. was 0.37 MPa, while the within-sensor S.D. was 0.22–0.27 MPa, or approximately 60–70% of the between-sensor value. This suggests that a large portion of the between-sensor variability was actually due

Table 5 – Regression equations and fit statistics for relating SSPS PSSI to SCPS PSSI

Site	Equation	n	r^2	S.E. (MPa)
All	SSPS PSSI = 0.83 × (SCPS PSSI) + 0.44	719	0.56	0.28
1	SSPS PSSI = 0.89 × (SCPS PSSI) + 0.35	528	0.66	0.24
2	SSPS PSSI = 0.72 × (SCPS PSSI) + 0.61	191	0.37	0.37

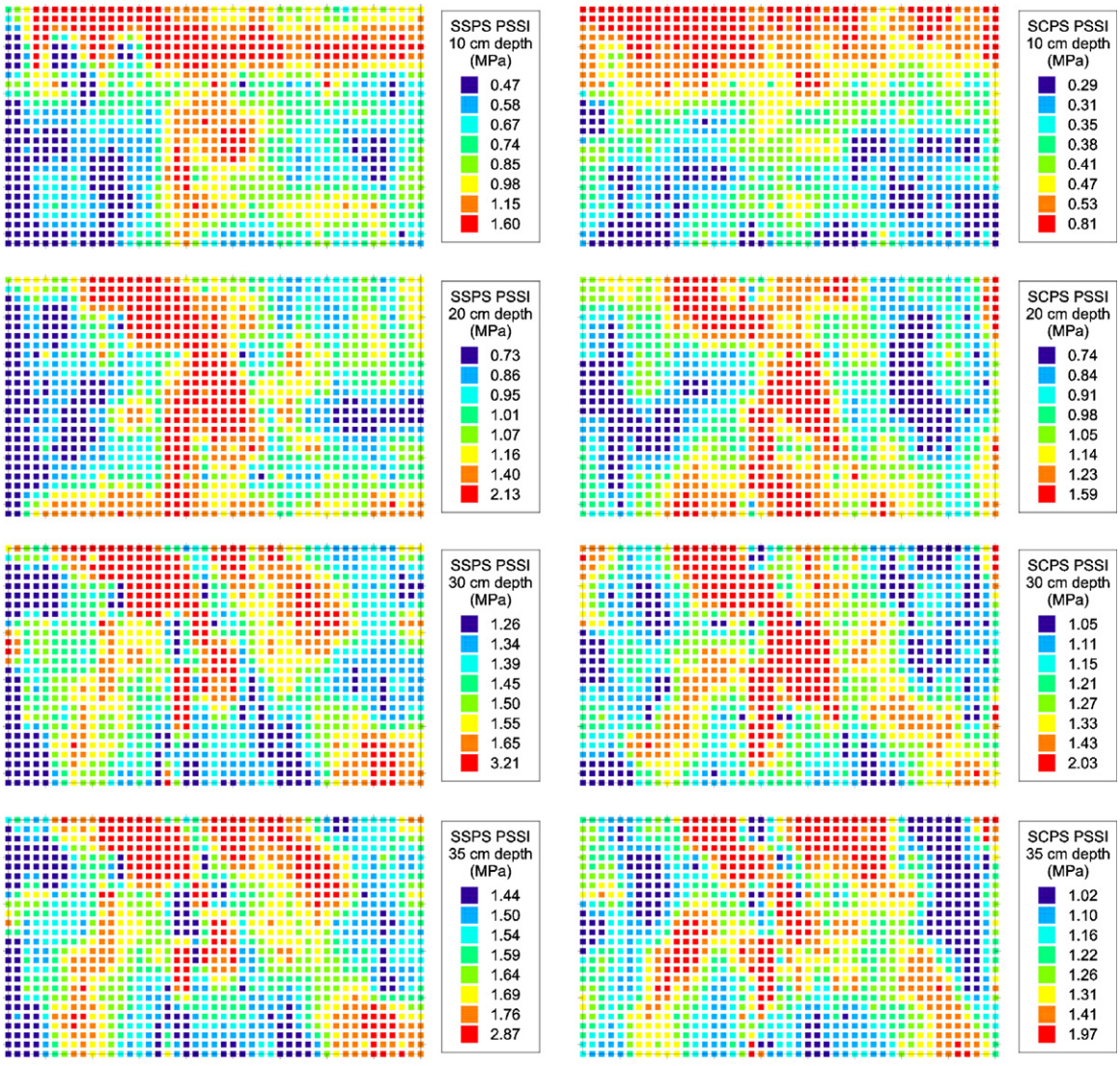

Fig. 7 – Mapped soil strength data (PSSI) obtained with soil compaction profile sensor (SCPS, right) and soil strength profile sensor (SSPS, left) for four sensing depths at site 1. Within each map, an equal-area color scale is used.

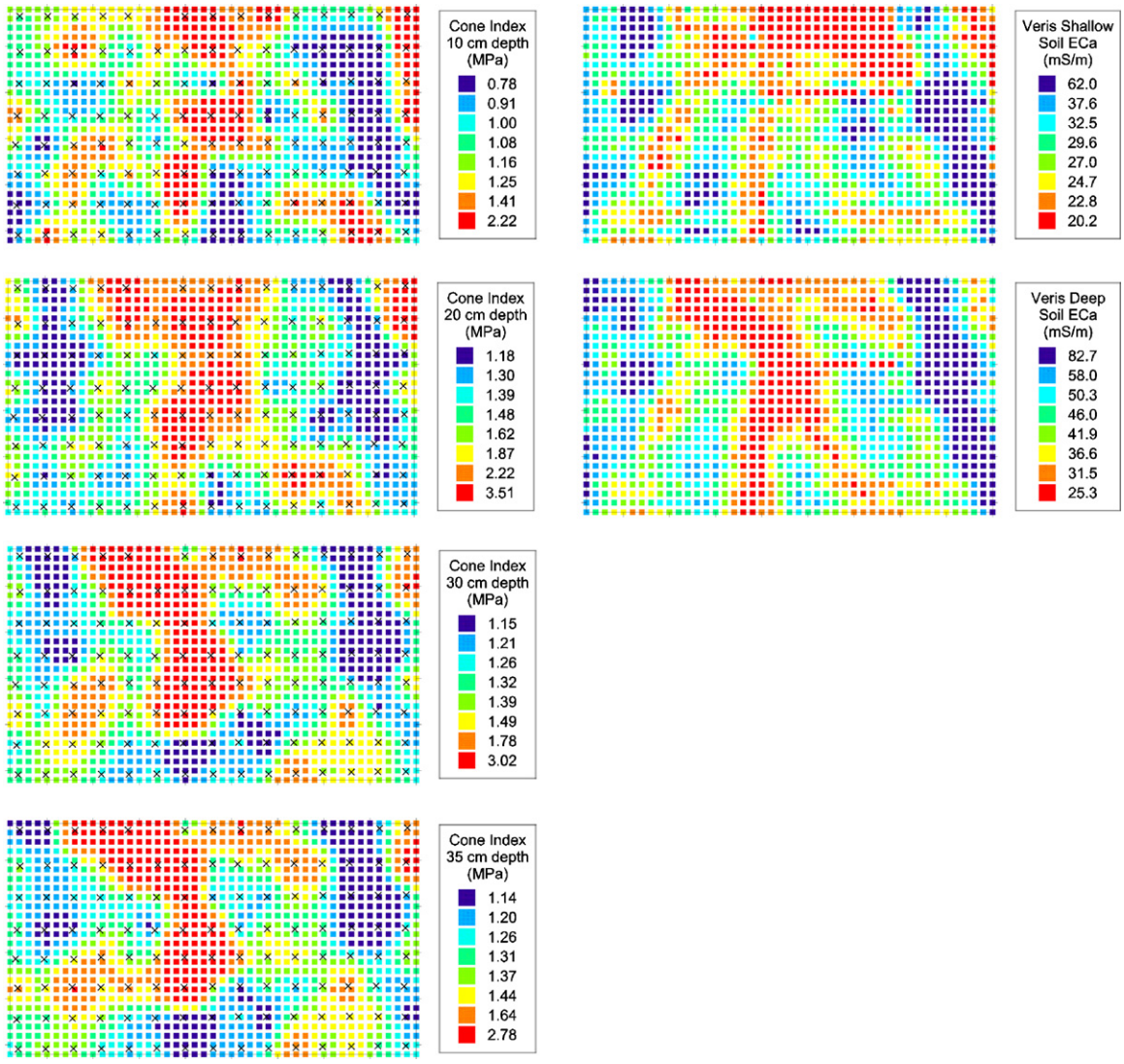

Fig. 8 – Mapped penetrometer cone index (CI) for four sensing depths at site 1 (left), and Veris 3100 shallow and deep soil electrical conductivity (EC_a), also for site 1 (right). Within each map, an equal-area color scale is used.

to soil differences at the scale of the spacing between measurement transects. Thus, the true difference in PSSI readings between the two sensors would be expected to be considerably less than 0.37 MPa if it were possible to sense the same location in the soil with both units.

3.3. *Comparison of field-scale soil strength maps*

A typical use of data from a soil strength sensor would be to develop field compaction maps that could be used for management planning and evaluation and/or to guide site-specific compaction remediation (e.g., deep tillage). Fig. 7 shows maps of soil strength, quantified as PSSI, for site 1. Because a separate equal-area color scale was used for the map representing each sensor–depth combination, direct comparison of compaction levels between maps based on color alone was not possible. However, the choice of the equal-area scale did facilitate comparison of spatial patterns in the data. Areas of higher and lower PSSI were very similar between the two sensors at each depth. As shown by correlation data in Table 4, the agreement was somewhat poorer for the 10-cm depth where soil strength was generally lower. Factors contributing to this difference may have included the lower sensing resolution of the SSPS as compared to the SCPS and differences in soil failure behavior at this depth.

For comparison, CI maps from site 1 are shown in Fig. 8, where sampling locations for CI are denoted by "x" symbols. With the exception of the 10-cm depth, all CI maps appear similar to the on-the-go sensor maps of Fig. 7. As discussed in Section 3.2, the difference at 10 cm may be due to crescent soil failure occurring with the SSPS and SCPS at this sensing depth. Additionally, soil properties at this shallow depth may have been more variable between the sensor transects due to soil cracking, residue incorporation, or other near-surface effects. As expected, the denser spatial data available from the on-the-go sensors capture more spatial detail than

is possible with CI mapping on the 30-m grid used in this study.

It appeared that most of the mapped spatial patterns in soil strength seen at site 1 were caused by intrinsic soil variation rather than by management operations (i.e., wheel traffic or tillage). Maps of Veris 3100 shallow (0–30 cm) and deep (0–100 cm) EC_a shown in Fig. 8 appear quite similar to the PSSI and CI maps. Higher EC_a indicated higher clay content and higher soil water content. At the time of data collection, the soil profile was fairly dry in areas of low EC_a, and relatively wetter at depth in areas of higher EC_a, resulting in higher PSSI in low EC_a areas.

One area where management may have affected soil strength was along the west boundary of the site. There, a flat, often wet end-row area was frequently compacted during harvesting operations. Higher soil strength measurements in this area were also reported previously in an intensive penetrometer study (Chung and Sudduth, 2004), and the locally high PSSI values seen here did not coincide with low EC_a. It may be that the data collection and processing approaches used in this study missed other areas of management-induced compaction, particularly if they were quite localized. Additional data collection and analysis would be needed to determine if localized features, such as compaction induced by as a single set of wheel tracks, could be successfully resolved and quantified with the on-the-go sensors.

4. Summary and conclusions

This research compared the field performance of two on-the-go soil strength sensors through tests conducted in two central Missouri field sites. Soils at the sites ranged from sandy loam to clay. The SSPS measured compaction to a 50-cm depth on 10-cm intervals; the SCPS recorded data to 40.6 cm on a 7.6-cm interval. Data obtained with each sensor on adjacent transects were well distributed around the 1:1 line with relatively low variability, indicating good repeatability of sensor measurements. The repeatability of SCPS data (S.E. = 0.20 MPa) was somewhat better than that of SSPS data (S.E. = 0.26 MPa), perhaps due to its higher sensing resolution at shallow depths and/or the larger base area of its sensing elements. Data from the two sensors were linearly related, with similar relationships found for each individual site and for both sites combined. The agreement between SCPS and SSPS data ($r^2 = 0.56$ over all sites and depths) was much better than between sensor and CI data ($r^2 = 0.19$ to 0.20). Similar to previous research, CI was more strongly related to on-the-go sensor data within a single depth than across depths, indicating that this relationship was depth-dependent. Maps of SCPS and SSPS data for a 13.5-ha field site showed very similar patterns. Maps of CI were also similar to those of on-the-go sensor data, but showed less spatial detail. Variation in soil strength appeared to be primarily related to variations in soil physical properties (e.g., texture and water content). Due to the similarity between SCPS and SSPS data, we conclude that the two on-the-go soil sensors were affected similarly by soil strength variations within the study sites.

Acknowledgements

This research was supported in part by the North Central Soybean Research Program, the United Soybean Board, the International Cooperative Research Program, Rural Development Administration, Republic of Korea, and the University of California Institute for Mexico and the United States (UC MEXUS). The authors express appreciation for the contributions of C. Plouffe, B. Poutre, S.T. Drummond, R.L. Mahurin, D.B. Myers, J. Sung, and M.R. Volkmann to field data collection and analysis.

REFERENCES

Adamchuk, V.I., Morgan, M.T., Sumali, H., 2001. Application of a strain gauge array to estimate soil mechanical impedance on-the-go. Trans. ASAE 44 (6), 1377–1383.

Alihamsyah, T., Humphries, E.G., Bowers Jr., C.G., 1990. A technique for horizontal measurement of soil mechanical impedance. Trans. ASAE 33 (1), 73–77.

Andrade-Sanchez, P., Upadhyaya, S.K., Jenkins, B.M., 2007. Development, construction, and field evaluation of a soil compaction profile sensor. Trans. ASABE 50 (3), 719–725.

Andrade, P., Upadhyaya, S.K., Jenkins, B.M., Plouffe, C., Poutre, B., 2004. Field Evaluation of the Improved Version of the UC Davis Compaction Profile Sensor (UCD-CPS). ASAE Paper No. 041037, ASAE, St. Joseph, MI.

ASAE, 2005a. Soil Cone Penetrometer. ASAE Standard S313.3, ASAE, St. Joseph, MI.

ASAE, 2005b. Procedures for Using and Reporting Data Obtained With the Soil Cone Penetrometer. ASAE Standard EP542, ASAE, St. Joseph, MI.

Busscher, W.J., Sojka, R.E., Doty, C.W., 1986. Residual effects of tillage on coastal plain soil strength. Soil Sci. 141 (2), 144–148.

Canarache, A., 1991. Factors and indices regarding excessive compactness of agricultural soils. Soil Tillage Res. 19 (2-3), 145–164.

Chukwu, E., Bowers, C.G., 2005. Instantaneous multiple-depth soil mechanical impedance sensing from a moving vehicle. Trans. ASAE 48 (3), 885–894.

Chung, S.O., Sudduth, K.A., 2004. Characterization of cone index and tillage draft data to define design parameters for an on-the-go soil strength profile sensor. Agric. Biosystems Eng. 5 (1), 10–20.

Chung, S.O., Sudduth, K.A., 2006. Soil failure models for vertically operating and horizontally operating strength sensors. Trans. ASABE 49 (4), 851–863.

Chung, S.O., Sudduth, K.A., Plouffe, C., Kitchen, N.R., 2004. Evaluation of an On-The-Go Soil Strength Profile Sensor Using Soil Bin and Field Data. ASAE Paper No. 041039, ASAE, St. Joseph, MI.

Chung, S.O., Sudduth, K.A., Hummel, J.W., 2006. Design and validation of an on-the-go soil strength profile sensor. Trans. ASABE 49 (1), 5–14.

Elbanna, E.B., Witney, B.D., 1987. Cone penetration resistance equation as a function of the clay ratio, soil moisture content and specific weight. J. Terramech. 24 (1), 41–56.

Glancey, J.L., Upadhyaya, S.K., Chancellor, W.J., Rumsey, J.W., 1989. An instrumented chisel for the study of soil-tillage dynamics. Soil Tillage Res. 14 (1), 1–24.

Glancey, J.L., Upadhyaya, S.K., Chancellor, W.J., Rumsey, J.W., 1996. Prediction of agricultural implement draft using an instrumented analog tillage tool. Soil Tillage Res. 37 (1), 47–65.

Godwin, R.J., Spoor, G., 1977. Soil failure with narrow tines. J. Agric. Eng. Res. 22 (4), 213–228.
Guerif, J., 1994. Effects of compaction on soil strength parameters. In: Soane, B.D., Van Ouwerkerk, C. (Eds.), Soil Compaction in Crop Production, 9. Elsevier, Amsterdam, pp. 191–214.
Hall, H.E., Raper, R.L., 2005. Development and concept evaluation of an on-the-go soil strength measurement system. Trans. ASAE 48 (2), 469–477.
Johnson, C.K., Doran, J.W., Duke, H.R., Wienhold, B.J., Eskridge, K.N., Shanahan, J.F., 2001. Field-scale electrical conductivity mapping for delineating soil condition. Soil Sci. Soc. Am. J. 65, 1829–1837.
Luth, H.J., Wismer, R.D., 1971. Performance of plane soil cutting blades in sand. Trans. ASAE 14 (2), 255–259, 262.
McKyes, E., 1985. Soil Cutting and Tillage. Elsevier, Amsterdam.
Mulqueen, J., Stafford, J.V., Tanner, D.W., 1977. Evaluating penetrometers for measuring soil strength. J. Terramech. 14 (3), 137–151.
Perumpral, J.V., 1987. Cone penetrometer applications – a review. Trans. ASAE 30 (4), 939–943.
Schuring, D.J., Emori, R.I., 1964. Soil Deforming Processes and Dimensional Analysis. SAE Paper No. 897C, SAE, New York, NY.
Soane, B.D., Van Ouwerkerk, C., 1995. Implications of soil compaction in crop production for the quality of the environment. Soil Tillage Res. 35, 5–22.
Sojka, R.E., Busscher, W.J., Lehrsch, G.A., 2001. In situ strength, bulk density, and water content relationships of a Durinodic Xeric Haplocalcip soil. Soil Sci. 166 (8), 520–529.
Stafford, J.V., 1979. The performance of a rigid tine in relation to soil properties and speed. J. Agric. Eng. Res. 24 (1), 41–56.
Sudduth, K.A., Kitchen, N.R., Bollero, G.A., Bullock, D.G., Wiebold, W.J., 2003. Comparison of electromagnetic induction and direct sensing of soil electrical conductivity. Agron. J. 95 (3), 472–482.
Sudduth, K.A., Hummel, J.W., Drummond, S.T., 2004. Comparison of the Veris Profiler 3000 to an ASAE-standard penetrometer. Appl. Eng. Agric. 20 (5), 535–541.
Wheeler, P.N., Godwin, R.J., 1996. Soil dynamics of single and multiple tines at speeds up to 20 km/h. J. Agric. Eng. Res. 63, 243–250.
Wismer, R.D., Luth, H.J., 1972. Performance of plane soil cutting blades in clay. Trans. ASAE 15 (2), 211–216.